Research on Cooperative Task Assignment of Multi-Agent Track Bolt Operation Robot Based on Optimized Multi-Objective Particle Swarm Optimization

Yanni Shen[1][a], Jianjun Meng[1,2,3,4,*][b], Defang Lv[1][c], Gaoyang Meng[1][d] and Zhicheng Wang[1][e]
[1]*School of Mechanical Engineering, Lanzhou Jiaotong University, Lanzhou 730070, China*
[2]*Institute of Mechanical and Electrical Technology, Lanzhou Jiaotong University, Lanzhou 730070, China*
[3]*Gansu Engineering Technology Research Center of Logistics and Transportation Equipment Informatization, Lanzhou 730070, China*
[4]*Gansu Logistics and Transportation Equipment Industry Technology Center, Lanzhou 730070, China*
*

Keywords: Multi-Agent, Track Bolt, Unmanned Vehicles, Task Assignment, Cooperative Control.

Abstract: To improve the efficiency of single-person, single-machine track bolt maintenance during railway skylight periods, we propose a collaborative task assignment control method using a multi-agent track bolt operation robot. A control decision model is developed with constraints on operation time and distance, aiming to optimize both total collaborative operation distance and completion time. By incorporating equations for robot speed and operation time, we derive the Pareto solution set for multi-agent task assignment. The method's effectiveness is verified through an enhanced particle evolution technique within the multi-objective particle swarm optimization (MOPSO) algorithm, and its performance is compared with that of standard MOPSO. Simulations in a real-world track bolt maintenance environment show that this approach produces a higher-quality Pareto solution set for task assignment.

1 INTRODUCTION

As railway construction in China accelerates, daily track maintenance has become increasingly essential. The condition of track bolts, a critical component of the track structure, directly impacts train safety and stability. However, the current single-person maintenance method during skylight periods is labor-intensive, inefficient, and poses safety risks. Thus, developing an efficient Multi-Agent Track Bolt Operation Robot (MATBOR) is imperative. In alignment with the "Digital Railway Planning" initiative by China National Railway Group Co., Ltd., we aim to achieve comprehensive digitalization and intelligence in railway operations, thereby enhancing modernization efforts. Improving intelligent maintenance equipment for track bolts is crucial.

This article addresses the collaborative task assignment problem for Multi-Agent Track Bolt Operation Robots (MATBOR), a typical NP-hard challenge marked by high computational complexity and long processing times (Li et al., 2022).

The Particle Swarm Optimization (PSO) algorithm is recognized for its high efficiency, simplicity, and quick convergence, making it ideal for solving single-objective optimization problems. However, it is not naturally suited for multi-objective optimization. Consequently, improving PSO for multi-objective tasks has become a significant research focus. Many researchers have extended the original algorithm and implemented various improvements to enhance the performance of the Multi-Objective Particle Swarm Optimization (MOPSO) algorithm (Figueiredo et al., 2016; Lv et al., 2016; Zhou et al., 2022; Sunet al., 2024; Wang and

[a] https://orcid.org/0009-0006-7316-3806
[b] https://orcid.org/0000-0001-6856-2577
[c] https://orcid.org/0009-0004-6779-2521
[d] https://orcid.org/0000-0002-2973-7976
[e] https://orcid.org/0009-0008-1531-9547

Shen, Y., Meng, J., Lv, D., Meng, G., Wang and Z.
Research on Cooperative Task Assignment of Multi-Agent Track Bolt Operation Robot Based on Optimized Multi-Objective Particle Swarm Optimization.
DOI: 10.5220/0013632100004671
In *Proceedings of the 7th International Conference on Environmental Science and Civil Engineering (ICESCE 2024)*, pages 248-256
ISBN: 978-989-758-764-1; ISSN: 3051-701X

Liu, 2016; Khan et al., 2016; Wang et al., 2021).

For instance, Liu et al. proposed a co-evolutionary PSO algorithm that employs synthetic immune principles, dividing the population into elite and ordinary subpopulations, which co-evolve for improved convergence and global search abilities (Liu et al., 2013). Goh et al. introduced a collaborative evolution paradigm that combines competition and cooperation to simultaneously tackle static and dynamic multi-objective problems (Goh and Tan, 2009). Song et al. developed a collaborative evolutionary PSO algorithm based on a bottleneck objective instructional strategy, maintaining diversity through distributed collaboration across multiple populations (Song et al., 2020). Huang et al. proposed a dual-phase multi-task allocation approach utilizing Discrete Particle Swarm Optimization (TMA-DPSO), which iteratively updates particle positions and velocities to enhance solutions (Huang et al., 2022). Lastly, Li et al. proposed a gBest strategy, utilizing a newly defined virtual generation distance index, to enhance search efficiency (Li et al., 2023).

Building on this foundation, This study introduces a method for task assignment in MATBOR, utilizing an optimized MOPSO algorithm. The key innovations of this study include:

(1) A two-stage subsampling method is implemented to improve the algorithm's convergence speed and accuracy.

(2) To address issues such as high computational complexity, limited diversity in Pareto optimal solutions, and challenges in handling complex constraints, this study employs a simple adaptive grid method to optimize the multi-objective particle swarm optimization algorithm, thereby enhancing its efficiency.

(3) Applying a collaborative task assignment method to MATBOR to enhance maintenance efficiency during railway skylight periods.

2 METHODOLOGY

2.1 Collaborative Task Assignment Model for Multi-Agent Rail Bolt Operation Robot

2.1.1 Problem Description

The collaborative task assignment problem for a multi-agent rail bolt operation robot system can be described as follows: assuming there are m MATBORs operating during a specific skylight period, represented by the robot set $R=\{r_1,r_2,r_3,r_4,\ldots\ldots,r_m\}$. if the range of the rail bolt area to be serviced does not exceed L_{max} and n bolts need to be maintained, the task set T can be represented as $T=\{t_1,t_2,t_3,t_4,\ldots\ldots,t_n\}$. Here, r_i represents the task assignment for the ith robot, $i\in[1,m]$; t_j represents the jth task to be assigned, $j\in[1,n]$. The working time during the skylight period must not exceed T_{max}. As shown in Figure 1, the central control center sends the specific areas and kilometers that require maintenance to the signal receiving station, which then relays these requirements to the monitoring operation screen used by the maintenance personnel and the MATBORs during the window period. Once the MATBORs begin working, they transmit the status of each completed task and equipment information to the signal receiving station in real-time. The maintenance work during the skylight period is considered successfully completed when all MATBORs have finished their assigned tasks simultaneously.

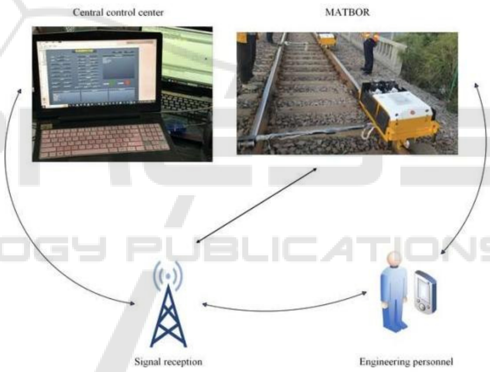

Figure 1: Schematic Diagram of Task Assignment for MATBOR.

2.1.2 Constraints

The MATBOR collaborative task assign-ment model includes the following key constraints:

(1) Task Coordination Constraints

To ensure that no task is executed multiple times or left unexecuted, task coordination constraints are incorporated into the model. This requires that each task must be executed exactly once and can only be assigned to a sing-le robot, as expressed in equation (1).

$$\sum_{i=1}^{n} x_{ij}=1 \qquad \forall j\in T \tag{1}$$

x_{ij} represents the assignment of tasks; n represents total number of tasks.

(2) Robot Coordination Constraints

To prevent errors in task execution, the model includes constraints for robot coordination. These constraints guarantee that each robot can undertake only one task at a t-ime during the assignment process, as illustrated in equation (2).

$$\sum_{j=1}^{m} x_{ij} = 1 \qquad \forall i \in R \tag{2}$$

m represents total number of multi-agent systems.

(3) Task Status

The variable representing whether the task t_j is assigned to the robot r_i is defined as follows: if the task is assigned to the robot, then: $x_{ij} = 1$; if the task is not assigned to the robot, then: $x_{ij} = 0$. As shown in equation (3).

$$x_{ij} \in \{0,1\} \quad \forall i \in R, \quad \forall j \in T \tag{3}$$

(4) Homework

All robots begin from the same starting point, and the bolts are sequentially numbered 1, 2, 3... n starting fro-m that origin.

(5) Operation Time and Distance Constraints

Given the time and distance limitations for maintenance work during the skylight period, the assigned MATBOR must not exceed the specified time, and the total distance traveled by a single robot must remain within the maximum allowable distance. These constraints are express-ed in equations (4) and (5).

$$\sum_{i=1}^{m} T_i \le T_{max} \tag{4}$$

$$D_i \le L_{max} \tag{5}$$

Were: $T_i = \left[\frac{\left(N_{ij}^S + 1\right)\cdot \Delta}{v_s} + \frac{\left(\left(N_{ij}^E - N_{ij}^S\right)+1\right)\cdot \Delta}{v_w} t_j \right] x_{ij}$,

$D_i = \sum_{j=1}^{n} \left| P_{r_i} - P_{t_j} \right| \cdot x_{ij}$

Where, T_i represents robot r_i completes task assignment and running time; D_i represents robot r_i total travel distance; T_{max} represents robot r_i maximum running time; L_{max} represents robot r_i maximum driving distance; N_{ij}^S and N_{ij}^E represent complete the starting and ending bolt numbers of the task separately; V_s represents ground speed: $V_s = 2m/s$; V_w represents operating speed: $V_w = 0.45m/s$; t_j represents task j execution time; P_{r_i} represents initial position: $P_{r_i} = (x_{r_i}, y_{r_i})$; P_{t_j} represents task element coordinates: $P_{t_j} = (x_{t_j}, y_{t_j})$.

2.1.3 Objective Function

To more effectively evaluate the task assignment results for the rail bolt robot, this model uses two objective functions: MATBOR task duration and overall travel distance.

Task completion time refers to the duration required to complete the final task in the maintenance process, while total travel distance refers to the sum of all distances traveled by the track bolt robots during the skylight period. The corresponding calculation formulas are given in equations (6) and (7).

$$F_1 = max \sum_{i=1}^{m} T_i \tag{6}$$

$$F_2 = \sum_{i=1}^{m} D_i \tag{7}$$

In equations (6) and (7), F_1 indicates the total time needed to finish the final task in the complete maintenance process, which corresponds to the maximum task completion time. F_2 represents the sum of the travel distances of all participating rail bolt robots across all systems. Since the goal is for the rail bolt robots to complete tasks as quickly as possible while minimizing resource consumption during task assignment, the model put forward in this paper considers both optimization objectives: minimizing F_1 and F_2 simultaneously. Based on these two objectives, the optimal objective function for MATBOR collaborative task assignment is formulated in equation (8).

$$z = min[F_1, F_2] \tag{8}$$

The MATBOR collaborative task assignment model involves both discrete and continuous variables, which complicates the solution space and makes it more difficult to search effectively. Additionally, the model includes multiple complex constraints, such as inequality and equality constraints, further increasing the irregularity of the solution space and the difficulty in finding feasible solutions. To tackle the challenges of multi-objective and multi-constraint collaborative task assignment in MATBOR, this paper introduces MOPSO algorithm that incorporates a quadratic sampling adaptive grid to address the multi-MATBOR collaborative task assignment challenge.

2.2 Multi-Objective PSO Based on Quadratic Sampling Adaptive Grid

2.2.1 Pareto Optimal Solution

Given the multiplicity and complexity of different objective functions, it is usually impossible for all objectives to reach their maximum or minimum values simultaneously. As a result, multi-objective optimization problems rarely have a single optimal solution. However, practical problems require decision-making to identify the best possible solution. To address this, Pareto optimal solutions are utilized to assess and balance conflicting objectives.

In multi-objective optimization, several objectives are optimized simultaneously. A solution is considered Pareto optimal if no objective can be enhanced without negatively impacting another (Lu et al., 2024). For two decision vectors x and y, if x dominates y, denoted as $x \prec y$, this means that x is no worse than y in all objectives, and enhanced in at least one objective.

A decision vector x is considered a Pareto optimal solution if no other vector in the objective space can dominate it. The group of all these solutions constitutes the Pareto optimal set (PS), while its graphical depiction is referred to as the Pareto optimal frontier (PF). According to the definition, enhancing one objective in a Pareto optimal solution necessarily diminishes at least one other. In multi-objective optimization, this collection is commonly known as the non-dominated solution set. The algorithm proposed in this paper aims to identify the Pareto optimal solution set, thereby enhancing the efficiency and balance of MATBOR task assignment.

2.2.2 Secondary Sampling

The more particle samples selected in the state space, the higher the approximation accuracy becomes (Liu, 2017). To address the issue where the weights of certain particles may reduce the effective sample space after multiple iterations, thereby affecting estimation accuracy, the quadratic sampling method has been introduced (Douc and Cappe, 2005). During the resampling process, particles with higher weights are duplicated, while those with lower weights are discarded, ensuring the particle count remains constant. Various subsampling methods exis (Li et al., 2015).

2.2.3 Improved Multi-Objective Particle Swarm Optimization Algorithm

The PSO algorithm, developed by Kennedy and Eberhart in 1995, is a swarm intelligence technique modeled after birds' food-searching behavior. It is especially adept at addressing complex, nonlinear continuous optimization challenges (Kennedy and Eberhart, 1995). Over time, PSO has been enhanced and adapted to tackle discrete problems as well. These improvements have expanded its applicability, enabling it to effectively address NP-hard problems, combinatorial optimization, and multi-objective optimization challenges, while also incorporating global guidance techniques (Yan et al., 2015; Gao et al., 2023; Lu et al., 2023). In PSO, particles adjust their direction and velocity for the next iteration by considering both their individual flight history and shared information from the swarm, demonstrating collective intelligence. The particle update equations are provided in (9) and (10).

$$v_i(t+1) = \omega v_i(t) + c_1 r_1 (p_i(t) - x_i(t)) + c_2 r_2 (g(t) - x_i(t)) \quad (9)$$

$$x_i(t+1) = x_i(t+1) + v_i(t+1) \quad (10)$$

Equation (9) represents the velocity update formula, while equation(10) is the position update formula. In these equations: $v_i(t+1)$ is the new velocity of particle *i* at time *t*+1; $v_i(t)$ is the velocity of particle *i* at time *t*; ω is the inertia weight, which controls the influence of the particle's previous velocity on its current velocity; c_1 and c_2 are acceleration constants, representing the weights of individual cognition and group cognition, respectively; r_1 and r_2 are random numbers in the range [0,1], used to maintain randomness; $g(t)$ is the global best position, representing the optimal position found by the entire particle swarm; $x_i(t)$ is the current position of particle *i* at time *t* and $x_i(t+1)$ is the new position of particle *i* at time *t+1*.

This paper introduces a two-stage subsampling method to address the challenges of low solution accuracy and slow search speed during the middle and later phases of the PSO algorithm. In the first stage, particles are sampled from the search space, where those farther from the non-dominated solutions are discarded, and those closer are retained and replicated, enhancing convergence speed and accuracy. However, this may reduce particle diversity. To counter this, the second-stage sampling focuses on non-dominated particles, discarding high-density particles and replicating low-density ones to preserve diversity. Since the grid is updated only when extreme boundary particles appear in the storage set, the mesh size can sometimes grow too large during evolution, affecting performance. In the second stage, the target area is segmented into smaller regions via a grid, and particle density in each region is used for estimation. The grid size is adjusted adaptively based on particle evolution. This leads to the development of MOPSO algorithm that incorporates quadratic sampling and an adaptive grid (QSAGMOPSO), as depicted in the flowchart in Figure 2.

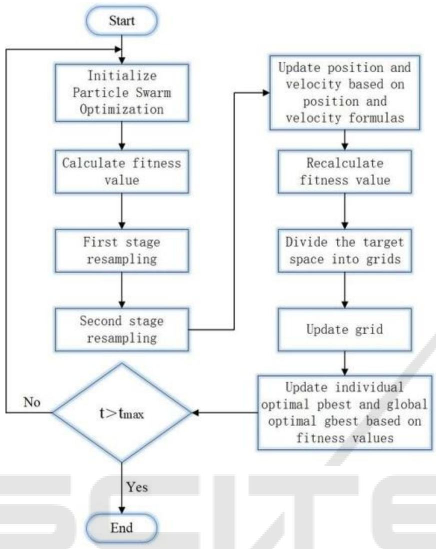

Figure 2: Flowchart of the Algorithm.

Step 1: Initialize the particle position data by dividing each dimension evenly, using these divisions as the initial coordinates in the decision space. To expand the distribution range, each dimension is divided according to its value range.

Step 2: Utilize the layered sampling method for secondary sampling. In the first stage, particles with higher weights are duplicated, while those with lower weights are discarded, maintaining a constant number of particles throughout the resampling process.

Step 3: Apply the secondary sampling method using a layered approach. In the initial stage, particles with greater weights are duplicated, while those with lesser weights are removed. The overall number of particles stays constant during the resampling process.

Step 4: Non-dominated solutions that meet the criteria are stored in an external file. When the file reaches its maximum capacity, new qualifying particles are added by screening the existing ones, ensuring the particle count remains constant.

Step 5: Determine the Pareto optimal solution set by assessing the fitness value of each particle for every objective. Analyze the dominance relationships between the particles, and collect all non-dominated solutions to form the current Pareto optimal set.

Step 6: Update each particle's velocity and position by applying the corresponding update formulas.

Step 7: Input the particle coordinates into each objective function and compute the corresponding function values.

Step 8: Utilize the adaptive grid method to compute the density of each particle in the Pareto optimal solution set. The search space is divided into smaller regions, with higher particle density indicating a greater number of particles within a grid. Low-density particles are replicated to preserve diversity.

Step 9: Using the historical data of each particle, identify the personal best particle (pbest) and the global best particle (gbest) based on their past fitness levels.

3 RESULTS

3.1 Experimental Comparison

To assess the feasibility and effectiveness of the QSAGMOPSO algorithm, benchmark problems ZDT1, ZDT2, and ZDT3 were selected for testing, with the details provided in Table 1. The population size was set to 400, with 200 generations of iterations and a file set size of 200. Each test was run 20 times, as shown in Figure 3. In the figure, red dots represent the true Pareto frontier, while green dots indicate the Pareto frontier identified by the QSAGMOPSO algorithm. A summary of the comparison results, including the mean and standard deviation for the ZDT functions, is provided in Table 1.

In the Table 1, variable range: $0 \le x_i \le 1$, $i = 1, 2, 3, \ldots, m$, $m = 30$.

Table 1: Benchmark Test Table.

Test questions	Objective Function
ZDT1	$f_1 = x_1$ $f_2 = g\left(1-\sqrt{\frac{f_1}{g}}\right)$ $g = 1+9\sum_{i=2}^{m}\frac{x_i}{m-1}$
ZDT2	$f_1 = x_1$ $f_2 = g(x)\left[1-\left(\frac{f_1(x)}{g(x)}\right)^2\right]$ $g = 1+\frac{9}{m-1}\sum_{i=2}^{m}x_i$
ZDT3	$f_1 = x_1$ $f_2 = g\left(1-\sqrt{\frac{f_1}{g}}-f_1/g\sin(10\pi f_1)\right)$ $g = 1+9\sum_{i=2}^{m}\frac{x_i}{m-1}$

As shown in Table 2, while various indicators can be used to assess two Pareto frontiers, no single measure is completely reliable. To address this, the paper employs two additional quality indicators, I_H and $I_{\in+}$, to compare algorithm performance. These indicators evaluate how closely the solutions align with the true Pareto front. Both I_H and $I_{\in+}$, range from 0 to 1, where higher I_H (or lower $I_{\in+}$) values indicate a better alignment with the true Pareto front. The results suggest that the proposed QSAGMOPSO algorithm outperforms the MOPSO algorithm.

Table 2: Performance Comparison Results of MOPSO and QSAGMOPSO on Benchmark Functions.

Problem		MOPSO		QSAGMOPSO	
		I_H	$I_{\in+}$	I_H	$I_{\in+}$
ZDT1	Mean	0.8907	0.1564	0.9093	0.1471
	Std.	0.0971	0.2790	0.0400	0.1806
ZDT2	Mean	0.6683	0.6500	0.8694	0.4520
	Std.	0.4927	0.2472	0.2668	0.2286
ZDT3	Mean	0.7420	0.3695	0.8122	0.1222
	Std.	0.8101	0.4553	0.8534	0.1813

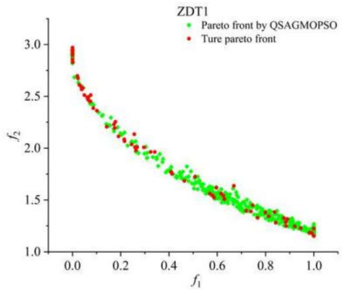

a

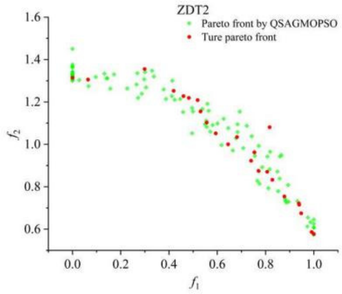

b

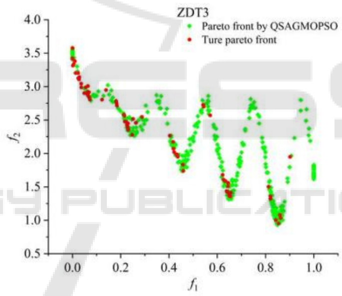

c

Figure 3: Pareto front of ZDT1, ZDT2, ZDT3.

3.2 Task Assignment Coding

Since the particle swarm optimization algorithm uses real number encoding, it cannot be directly applied to the discrete task assignment problem in MATBOR. Therefore, this paper adopts a method of truncating decimal places and retaining integer digits to decode the results obtained by the algorithm, effectively transforming the problem from a continuous domain into a discrete one. Assuming there are m rail bolt robots that need to perform n tasks during the skylight period, the assignment plan is expressed as an n-bit array $[t_1, t_2, t_3, \ldots, t_n]$. Each t_j in the array is a randomly generated number falling within the range $[1, m]$,and the integer part of t_j represents the id of the robot assigned to perform the *j*th task. Tasks with the same integer part are executed by the same rail bolt robot, while the decimal part is rounded during the encoding process.

For example, if there are three track bolt robots tasked with performing 300 jobs during the skylight period, the task assignment code arrangement is shown in Table 3.

Table 3: Example of Task Assignment Scheme.

Particle number	1 ⋯ 66	67 ⋯ 230	231 ⋯ 300
Robot coding	3	2	1

In this task assignment scheme, bolts numbered 1 to 66 are executed by Robot 3, bolts numbered 67 to 230 are handled by Robot 2, and bolts numbered 231 to 300 are assigned to Robot 1.

3.3 Example Simulation

A simulation was conducted in Matlab to address the task assignment problem for multi-agent rail bolt operation robots. The resulting comparison of the algorithm's performance is illustrated in Figure 4 and Figure 5.

From Figure 4 and Figure 5, it can be observed that both algorithms were run 20 times across different task quantity scenarios. Two multi-objective optimization algorithms were used to record all Pareto frontiers obtained in each instance. To further evaluate the Pareto solution sets, two metrics were introduced: Average Ratio (AR) and Spacing Metric (SP). The results of these evaluations are presented in Tables 4 and 5.

Table 4: Comparison of AR Values for Pareto Solution Sets of Two Algorithms.

Number of tasks	Number of robots	MOPSO	QSAGMOPSO
300	3	0.15	0.63
	5	0.37	0.77
	10	0.69	0.83
400	3	0.35	0.71
	5	0.57	0.85
	10	0.79	0.97

Table 5: Comparison of SP Values for Pareto Solution Sets of Two Algorithms.

Number of tasks	Number of robots	MOPSO	QSAGMOPSO
300	3	313.41	236.94
	5	302.43	259.13
	10	222.92	209.24
400	3	378.59	357.91
	5	347.45	323.25
	10	328.21	305.59

According to Tables 4 and 5, Table 4 compares the AR values of the two algorithms. In the instance tests, the AR values for the proposed QSAGMOPSO algorithm were consistently higher than those for the MOPSO algorithm, indicating that the QSAGMOPSO algorithm produces higher-quality solutions. Table 5 presents the average SP values for each scenario. Across all scenarios, the proposed QSAGMOPSO algorithm consistently achieved the lowest average SP values, reflecting better distribution and uniformity of solutions along the Pareto front.

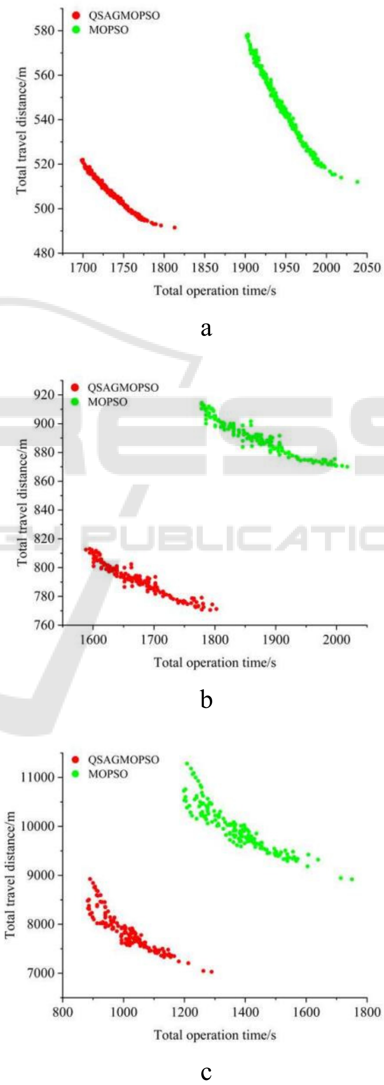

Figure 4: Comparison chart showing the completion of the same task(300 pieces) by different numbers of robots. a:3 robots; b:5 robots; c:10 robots.

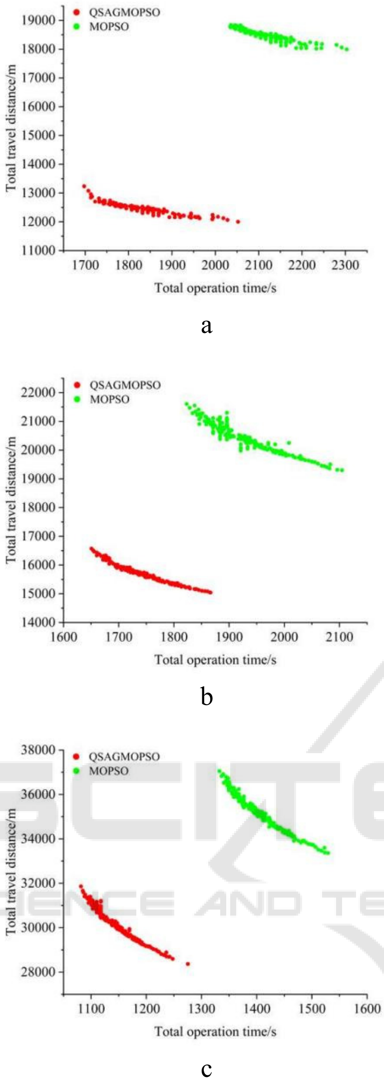

Figure 5: Comparison chart showing the completion of the same task(400 pieces) by different numbers of robots. a:3 robots; b:5 robots; c:10 robots.

4 CONCLUSION

In this article, we address a previously unexplored problem in multi-robot task assignment: the collaborative task assignment of multi-agent rail bolt operation robots. By introducing the concept of collaborative control from multi-agent systems into railway engineering, we redefine the fully automated rail bolt robot as an intelligent agent capable of independent decision-making. With a single instruction from a staff member, the robot can efficiently complete the heavy maintenance and engineering tasks of track bolts during the skylight period.

We further improved the classical multi-objective particle swarm optimization (MOPSO) algorithm by integrating quadratic sampling and a straightforward adaptive grid partitioning method. These enhancements tackle the problems of slow convergence and getting stuck in local optima during the later stages of the traditional PSO algorithm. The simulation results demonstrate that the task assignment method proposed in this paper greatly enhances task efficiency.

In future research, we will refine the constraints based on real-world engineering requirements and further develop the task assignment model to meet broader practical needs.

ACKNOWLEDGEMENTS

The authors acknowledge the support of Lanzhou Jiaotong University for this study.

REFERENCES

Li, J., Hua, N., Zhu, K., et al. 2022. Leveraging joint allocation of multidimensional resources for distributed task assignment. *J Opt Commun Netw*, 14(5): 351-364.

Figueiredo E M N, Ludermir, T. B., Bastos-Filho, C. J. A. 2016. Many objective particle swarm optimization. *Information Sciences*, 374: 115-134.

Lv, Z., Wang, L., Han, Z., et al. 2019. Surrogate-assisted particle swarm optimization algorithm with pareto active learning for expensive multi-objective optimization. *IEEE/CAA Journal of Automatica Sinica*, 6(3): 838-849.

Zhou, T., Long, Q., Law K M Y, et al. 2022. Multi-objective stochastic project scheduling with alternative execution methods: An improved quantum-behaved particle swarm optimization approach. *Expert Systems with Applications*, 203: 117029.

Sun, B., Zeng, Y., Zhu, D. 2024. Dynamic task allocation in multi autonomous underwater vehicle confrontational games with multi-objective evaluation model and particle swarm optimization algorithm. *Applied Soft Computing*, 153: 111295.

Wang, C.-F., Liu, K. 2016. A novel particle swarm optimization algorithm for global optimization. *Computational Intelligence and Neuroscience*, 2016(1): 9482073.

Khan, S. U., Yang, S., Wang, L., et al. 2016. A modified particle swarm optimization algorithm for global optimizations of inverse problems. *IEEE Transactions on Magnetics*, 52(3): 1-4.

Wang, F., Zhang, H., Han, M., et al. 2021. A mixed variable multi-objective particle swarm optimization algorithm based on collaborative evolution for solving unmanned aerial vehicle collaborative multi task allocation problem. *Journal of Computer Science*, 44 (10): 1967-1983.

Liu, Z. H., Zhang, J., Zhou, S. W., et al. 2013. Coevolutionary particle swarm optimization using ais and its application in multiparameter estimation of pmsm. *IEEE Transactions on Cybernetics*, 43(6): 1921-1935.

Goh, C. K., Tan, K. C. 2009. A competitive-cooperative coevolutionary paradigm for dynamic multiobjective optimization. *IEEE Transactions on Evolutionary Computation*, 13(1): 103-127.

Song, X. F., Zhang, Y., Guo, Y. N., et al. 2020. Variable-size cooperative coevolutionary particle swarm optimization for feature selection on high-dimensional data. *IEEE Transactions on Evolutionary Computation*, 24(5): 882-895.

Huang, M., Leung, V. C. M., Liu, A., et al. 2022. Tma-dpso: Towards efficient multi-task allocation with time constraints for next generation multiple access. *IEEE Journal on Selected Areas in Communications*, 40(5): 1652-1666.

Li, Y., Zhang, Y., Hu, W. 2023. Adaptive multi-objective particle swarm optimization based on virtual pareto front. *Information Sciences*, 625: 206-236.

Lu, K., Tang, K., Dong, S., et al. 2024. Generalized-nash-equilibrium-based pareto solution for transmission-distribution-coupled optimal power flow. *IEEE Transactions on Power Systems*, 39(2): 4051-4063.

Liu, B. 2017. Posterior exploration based sequential monte carlo for global optimization. *Journal of Global Optimization*, 69(4): 847-868.

Douc, R., Cappe, O. 2005. Comparison of resampling schemes for particle filtering. *ISPA 2005 Proceedings of the 4th International Symposium on Image and Signal Processing and Analysis*, 2005: 64-69

Li, T., Bolic, M., Djuric, P. M. 2015. Resampling methods for particle filtering: Classification, implementation, and strategies. *IEEE Signal Processing Magazine*, 32(3): 70-86.

Kennedy, J., Eberhart, R. 1995. Particle swarm optimization;. *Proceedings of ICNN'95 - International Conference on Neural Networks*, vol. 1944, pp. 1942-1948

Yan, J., Li, X., Liu, B. 2015. Application of Discrete Particle Swarm Optimization Guo Tao Algorithm for Multi UAV Collaborative Task Allocation [J] *Journal of National University of Defense Technology*, 37 (04): 165-171.

Gao, J., Tan, Y., Li, D., et al. 2023. Discrete particle swarm optimization algorithm for solving unrelated parallel machine scheduling problems with service life maintenance [J] *Computer Integrated Manufacturing System*, 1-18.

Lu, Y., Li, B., Liu, S., et al. 2023. A population cooperation based particle swarm optimization algorithm for large-scale multi-objective optimization. *Swarm and Evolutionary Computation*, 83: 101377.